6.1 Materials

Temozolomide (TMZ) was obtained as a gift sample from Cipla Ltd., Mumbai (India). Bovine serum albumin (BSA), chondroitin sulphate (CS), acetic acid, sodium acetate, sodium hydroxide, gluteraldehyde, N- hydroxysuccinimide (NHS), dialysis membrane (12000 Da cut-off), culture media, culture plates, culture flasks and transwell inserts were purchased from Himedia (India). Ethanol, hydrochloric acid, glacial acetic acid, phosphoric acid and N-Ethyl-N'-(3-dimethylaminopropyl) carbodiimide HCl (EDC) were purchased from Spectrochem Pvt Ltd, Mumbai (India). Hyaluronic acid (HA) was obtained as gift sample from Novozymes, Denmark. Hexadecyltrimethylammonium bromide (CTAB) and trehalose were purchased from SD Fine chemicals, Mumbai (India). HPLC grade acetonitrile and methanol were purchased from Renkem (India). Disodium hydrogen phosphate, potassium dihydrogen phosphate, sodium chloride, sodium acetate, sodium hydroxide, potassium sulphate, Tris-hydrochloride and dipotassium EDTA dihydrate were purchased from SD fine chemicals Pvt. Ltd., Mumbai, India. All other chemicals and solvents used were of analytical grade.

6.2 Equipments

- pH meter (Lab India Pvt. Ltd. India)
- Digital analytical balance (ATX224 Shimadzu, Japan)
- UV-Visible spectrophotometer (1800 Shimadzu, Japan)
- Cooling centrifuge (Remi equipment Pvt Ltd, India)
- Magnetic stirrer (Remi sci. Equipment, India)
- Deep freezer (EIE Inst. Ltd, Ahmedabad)
- Zetasizer (Nano ZS, Malvern ltd., UK)
- Differential Scanning Calorimeter (DSC-60-Shimadzu Corporation , Japan)
- Infrared Spectrophotometer (IR Affinity -1S,Shimadzu , Japan)
- Lyophilizer (Advantage 2.0 Bench Top Freeze Dryer/ Lyophilizer, SP Scientific, USA)

6.3 Methods

6.3.1 Surface modification of TNPs with Hyaluronic acid (HA)

HA was conjugated with TNPs by carbodiimide chemistry. In brief, 1 mole HA was dissolved in MES (2-(N-morpholino) ethane sulfonic acid) buffer (pH 4.7) and then EDC and NHS (2 mole each) were added and kept under stirring for 4 h. Subsequently, the mixture was incubated with TNPs under continuous stirring at room temperature. The conjugated HA-TNPs were collected by centrifugation at 15000 rpm for 30 min and washed thrice with water to remove excess HA. Percent conjugation efficiency of HA with TNPs was determined by CTAB turbidimetric method (refer section 3.10) (1,2).

6.3.2 Surface modification of TNPs with Chondroitin sulphate (CS)

CS was also conjugated with TNPs by carbodiimide chemistry (3) Briefly, CS, EDC and NHS at molar ratio of 1: 2: 2 were dissolved in 0.01 M MES (pH 4.7) to activate carboxylic groups of CS. Subsequently, TNPs were added in the mixture (CS: TNPs ratio = 1:1 w/w) and kept under continuous stirring for 12 h at RT. The conjugated CS-TNPs were separated by centrifugation at 15,000 rpm for 30 min and washed thrice with water to remove unreacted materials. Percent conjugation efficiency of CS with TNPs was determined by previously reported CTAB turbidimetric method (1)

6.3.3 Optimization of surface modified TNPs (HA-TNPs)

Conjugation of HA with TNPs was optimized by OVAT approach on the basis of effect of different variables like molecular weight of HA, stirring time and HA: TNPs ratio on quality attributes like size, PDI, zeta potential and % conjugation efficiency.

6.3.4 Optimization of surface modified TNPs (CS-TNPs)

Conjugation of CS with TNPs was optimized by OVAT analysis on the basis of effect of CS: TNPs ratio (1:1, 2:1 and 3:1) and stirring time (1 h, 2 h, 4 h and 12 h) on size, PDI, zeta potential and % conjugation efficiency.

6.3.5 Lyophilization of surface modified TNPs (HA-TNPs and CS-TNPs)

The surface modified TNPs (HA-TNPs and CS-TNPs) aqueous dispersion with 5 % w/w cryoprotectant (trehalose) was lyophilized using a lab freeze-dryer (Advantage 2.0 Bench Top Freeze Dryer/ Lyophilizer, SP Scientific, USA) as mentioned in section 5.3.5 (4).

6.3.6 Characterization of Surface modified TNPs (HA-TNPs and CS-TNPs)

6.3.6.1. Particle size and PDI determination

The particle size and PDI of Surface modified albumin nanoparticles (HA-TNPs and CS-TNPs) were determined with a Malvern Zetasizer (Nano ZS, Malvern ltd., UK) (please refer section 5.3.6.1) (5,6).

6.3.6.2. Zeta potential determination

The zeta potential of developed HA-TNPs and CS-TNPs were measured by determining the electrophoretic mobility using the Malvern Zetasizer (Nano ZS, Malvern ltd., UK) (please refer section 5.3.6.2) (5,6).

6.3.6.3. DSC analysis

DSC analysis of developed HA-TNPs and CS-TNPs were carried out using a Differential Scanning Calorimeter (DSC-60, Shimadzu, Japan) by the method described in section 5.3.6.3 (7).

6.3.6.4. FTIR analysis

FTIR spectrum of HA-TNPs and CS-TNPs were measured with a FTIR spectrophotometer (IR Affinity -1S (Shimadzu, Japan) in range 400–4000 cm^{-1} using a resolution of 4 cm^{-1} (7,8).

6.3.6.5. XRD analysis

X-ray diffraction patterns of HA-TNPs and CS-TNPs were obtained using X-ray diffractometer (RigakuUltima IV; Japan) by the method described in section 5.3.6.5 (6,7)

6.3.6.6. Morphology

Morphology of HA-TNPs and CS-TNPs were observed using transmission electron microscope (Philips CM200) (8).

6.3.7 Evaluation of Surface modified TNPs (HA-TNPs and CS-TNPs)

6.3.7.1. Estimation of entrapment efficiency and drug loading

TMZ entrapped in HA-TNPs and CS-TNPs were determined indirectly by measuring the amount of free TMZ in the supernatant using UV–visible spectrophotometer (Shimadzu UV-1700 at 330 nm (7). Then percentage entrapment efficiency (% EE) and drug loading (% DL) was determined using the formula:

$$\%EE = \frac{(\text{Total drug} - \text{Free drug})}{\text{Total drug}} \times 100 \qquad \text{……Equation 6.1}$$

$$\%DL = \frac{\text{Entraped drug}}{\text{Total weight of nanoparticles}} \times 100 \qquad \text{……Equation 6.2}$$

6.3.7.2. In-vitro drug release

The in-vitro drug release studies were carried out using dialysis bag method at 37 ℃ under mild stirring (50 rpm) (9). HA-TNPs and CS-TNPs (equivalent to 5mg drug) were taken into dialysis bags (MWCO = 12000), and were immersed into beakers containing 30 ml sodium acetate buffer (pH 5.5 ± 0.2). At predetermined period, 1.0 ml of sample was withdrawn and same quantity of fresh buffer was added into the beaker to maintain sink condition. The amount of TMZ released was determined using UV spectrophotometer at 330 nm. The obtained results were compared with the in –vitro release profile of pure TMZ and TNPs.

6.3.8 Bio-Interactions of Surface modified TNPs (HA-TNPs and CS-TNPs)

6.3.8.1. Interactions with plasma proteins

The interactions of HA-TNPs and CS-TNPS with plasma protein were studied to assess the bio-stability of the prepared nanoparticles. HA-TNPs and CS-TNPs in concentration of 5 mg/ml

were dispersed in PBS (pH 7.4) and mixed with protein solution (10% w/v) respectively and incubated at 37°C in orbital shaker. After 4 h, the mixture was centrifuged at 12000 rpm and obtained pellet was redispersed in double distilled water. Then particle size and zeta potential of nanoparticles dispersion (HA-TNPs and CS-TNPs) were measured (10,11).

6.3.8.2. Interactions with cell culture media (DMEM)

The interactions of HA-TNPs and CS-TNPs with DMEM media were studied by dispersing HA-TNPs and CS-TNPs (5 mg/ml) in PBS (pH 7.4) and mixed with DMEM media respectively and incubated at 37°C in orbital shaker. After 4 h, the mixture was centrifuged at 12000 rpm and obtained pellet was redispersed in double distilled water. Then particle size and zeta potential of nanoparticles dispersion (HA-TNPs and CS-TNPs) were measured (10,12).

6.3.8.3. Interactions with serum

The interactions of HA-TNPs and CS-TNPs with serum were studied by dispersing HA-TNPs and CS-TNPs (5 mg/ml) in PBS (pH 7.4) and mixed with 50% v/v serum respectively and incubated at 37°C in orbital shaker. After 4 h, the mixture was centrifuged at 12000 rpm and obtained pellet was redispersed in double distilled water. Then particle size and zeta potential of nanoparticles dispersion (HA-TNPs and CS-TNPs) were measured (11).

6.3.8.4. Haemolysis study

For haemolysis study, 1.0 ml blood sample was collected in EDTA solution (30 µl) containing eppendorf tube from the Sprague Dawley rat by retro-orbital puncture. Blood sample was then centrifuged at 5000 rpm for 10 min at 4 °C to separate the red blood cells (RBCs). The separated RBC pellet was re-suspended in normal saline and plasma components were removed by washing with normal saline (0.9 % w/w Sodium Chloride in water) 3 times before use. Then 0.5 % v/v RBCs were prepared by re-suspending RBC pellet (250 µl) in 50 ml of normal saline. Then 1 ml of RBCs was added to plain drug suspension, HA-TNPs and CS-TNPs containing 1mg equivalent amount of TMZ dispersed in 1ml of saline. For positive and negative control, 2.0% Triton-X100 (1ml) and 0.5% DMSO was used respectively. After treatment (with drug suspension, HA-TNPs, CS-TNPs, positive control and negative control), RBC dispersion was

gently stirred to uniformly disperse RBCs. The treated dispersions were stored at 37°C for 30 min in incubator. After incubation, all the samples were centrifuged at 3000 rpm for 12 min at 4 °C to separate the RBC mass and the solutions were analyzed for UV absorbance at λmax of 540 nm against normal saline as a reference solution (13,14). Percentage of haemolysis was determined using following equation:

$$\%\, Haemolysis = \left[\frac{A_{540}\ of\ sample - A_{540}\ of\ negative\ control}{A_{540}\ of\ positive\ control - A_{540}\ of\ negative\ control}\right] \times 100 \quad \text{……Equation 6.3}$$

6.3.9 Stability studies

The stability of the lyophilized HA-TNPs and CS-TNPs were investigated by storing samples at refrigerated condition (4°C) and at room temperature (25°C ±2°C) for 3 months. At regular time interval of 1 month, samples were withdrawn and checked for particle size, assay and zeta potential (15–17) .

6.3.10 Statistical Data Analysis

Results are given as mean ± SD. Statistical significance was tested by two-tailed Student's t test or one-way ANOVA. Statistical significance was set at $P < 0.05$.

6.4 Results and discussion

6.4.1 Conjugation of HA with TNPs (HA-TNPs)

HA was used as a targeting ligand to achieve CD44 receptor (over expressed in brain tumor cells) mediated targeting of brain tumor. HA was conjugated with TNPs using carbodiimide chemistry (figure 6.1). HA-TNPs optimization was done by varying single factor at a time and observing its effect on the different quality attributes like particle size, PDI, zeta potential and % conjugation of HA.

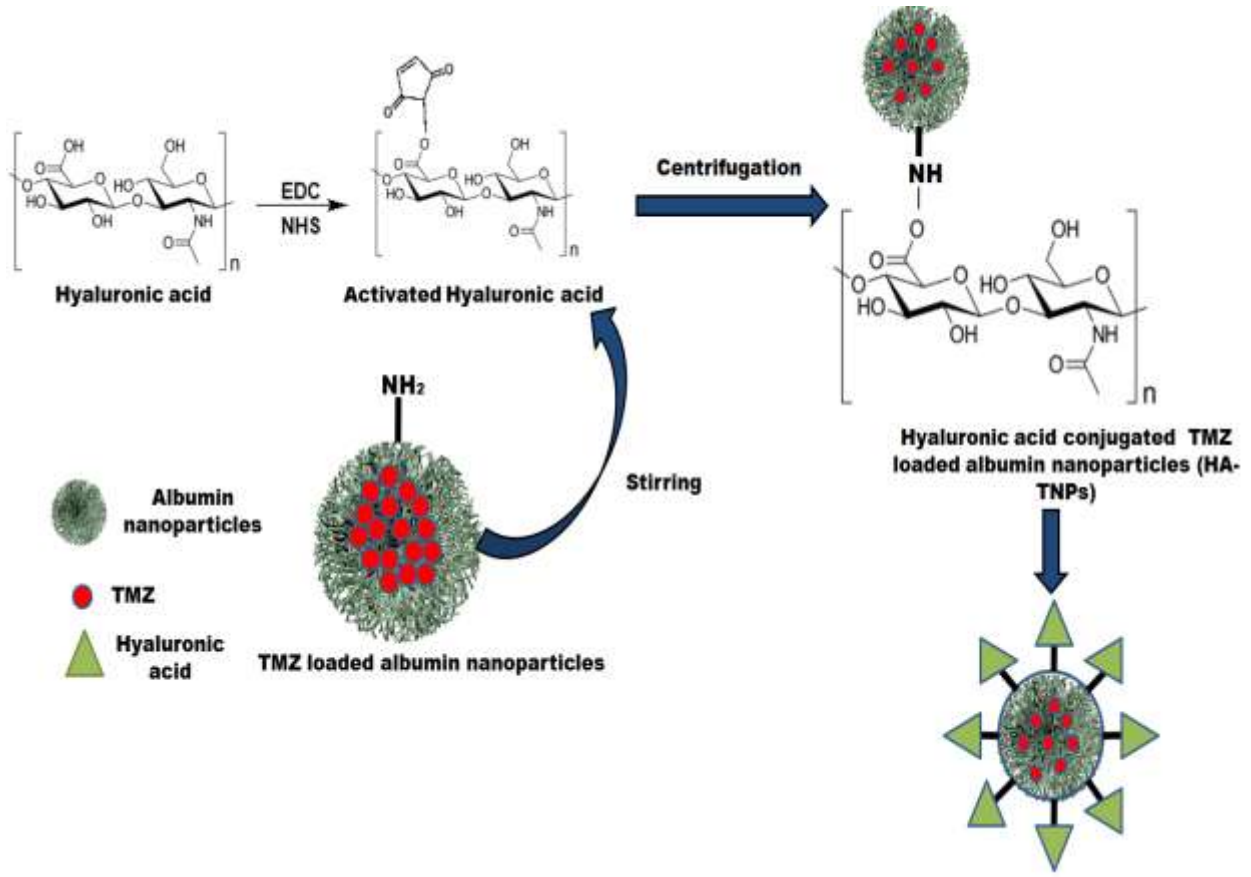

Figure 6.1: Schematic representation of preparation of HA-TNPs

6.4.1.1 Effect of molecular weight of HA on conjugation

Two different grades of HA (high molecular weight and low molecular weight) were used for conjugation purpose. For optimization, HA : NPs ratio (1:1) and stirring time for conjugation (45 min) was kept constant throughout the reaction. The results are shown in table 6.1 and figure 6.2A. High molecular weight (HMW) HA gave larger conjugated TNPs (1377 ± 1.8 nm) as compared to low molecular weight (LMW) HA (430.3 ± 1.4 nm).This may be correlated with the fact that higher molecular weight HA have longer hydrophilic chains which expanded in water and led to formation of larger particles. Although conjugation efficiency was found to be high with HMW HA (88.4 % ± 1.9 %) as compared to LMW HA (65.20 % ± 1.6 %), LMW HA was selected on the basis of size as size plays important role in cellular uptake and internalization. Cellular uptake of smaller particles is more as compared to larger particles (18).

Table 6.1: Effect of molecular weight of HA on conjugation

HA mol. Wt.	Particle size	PDI	Zeta potential	conjugation efficiency
High	1377.0 ± 1.7	0.522 ± 0.003	-43.1 ± 1.2	88.4 ± 1.9
Low	430.3 ± 1.3	0.185 ± 0.007	-38.8 ± 0.6	65.2 ± 1.5

6.4.1.2 Effect of HA : NPs ratio on conjugation

Two different HA : NPs ratios were selected to optimize HA-TNPs viz. 1:1 and 2:1. Obtained results as shown in table 6.2 and figure 6.2B indicated that HA : NPs ratio did not have significant effect on particle size, PDI and zeta potential but had significant effect on conjugation efficiency. The insignificant effect of HA: NPs ratio on particle size, PDI and zeta potential can be understood by the fact that the surface area of nanoparticles remains constant and so are the number of amine groups available on NPs to bind with carboxylic groups of HA. So, the increase in number of HA molecules will not affect the size, PDI and zeta potential to any large extent but in case of conjugation efficiency, it does play an important role. With more number of HA molecules, there will be more chances of its conjugation on NPs while with less molecules of HA, the conjugation on NPs will be less. So on the basis of higher conjugation efficiency, 1:1 was selected as HA: NPs ratio and used for further optimization.

Table 6.2: Effect of HA : NPs ratio on conjugation

HA : NPs	Particle size (nm)	PDI	Zeta potential (mV)	% conjugation efficiency
1:1	**430.3 ± 1.5**	**0.185 ± 0.005**	**-38.8 ± 0.5**	**65.2 ± 1.2**
2:1	**426.1 ± 1.75**	**0.250 ± 0.003**	**-35.2 ± 1.2**	**50.6 ± 1.9**

6.4.1.3 Effect of stirring time on conjugation

Stirring time is also a critical parameter which affects conjugation of HA with TNPs. The effect of stirring time on the conjugation at different time points (15 min - 60 min) on different quality attributes were observed (table 6.3 and figure 6.2C). Initially, larger particles were formed and after 30 min of stirring, particle size decreased and conjugation efficiency was increased. Formation of larger particles during initial stirring time may be due to lack of sufficient time for making conjugate which led to formation of unstable conjugate. As the stirring time increased, conjugation between HA and TNPs took place and led to formation of smaller particles having higher conjugation efficiency. With further increase in stirring time, particle size also increased and conjugation efficiency was decreased subsequently. This may be due to saturation of conjugating functional groups which led to only layering of HA over the TNPs rather than conjugation that caused only enhancement of particle size and decreased conjugation efficiency. Increase in particle size may also be due to swelling of HA in aqueous environment with time. Thus 30 min was selected as optimum stirring time for conjugation of HA with TNPs.

Table 6.3 Effect of stirring time on conjugation

Time (min)	Particle size (nm)	PDI	Zeta potential (mV)	% conjugation efficiency
15	436.2 ± 1.5	0.209 ± 0.005	-33.8 ± 1.5	67.4 ± 1.6
30	375.1 ± 1.7	0.181 ± 0.003	-33.6 ± 1.2	78.3 ± 1.9
45	430.3 ± 1.3	0.185 ± 0.007	-38.8 ± 1.5	65.2 ± 1.5
60	445.7 ± 1.2	0.194 ± 0.005	-37.8 ± 1.1	63.1 ± 1.8

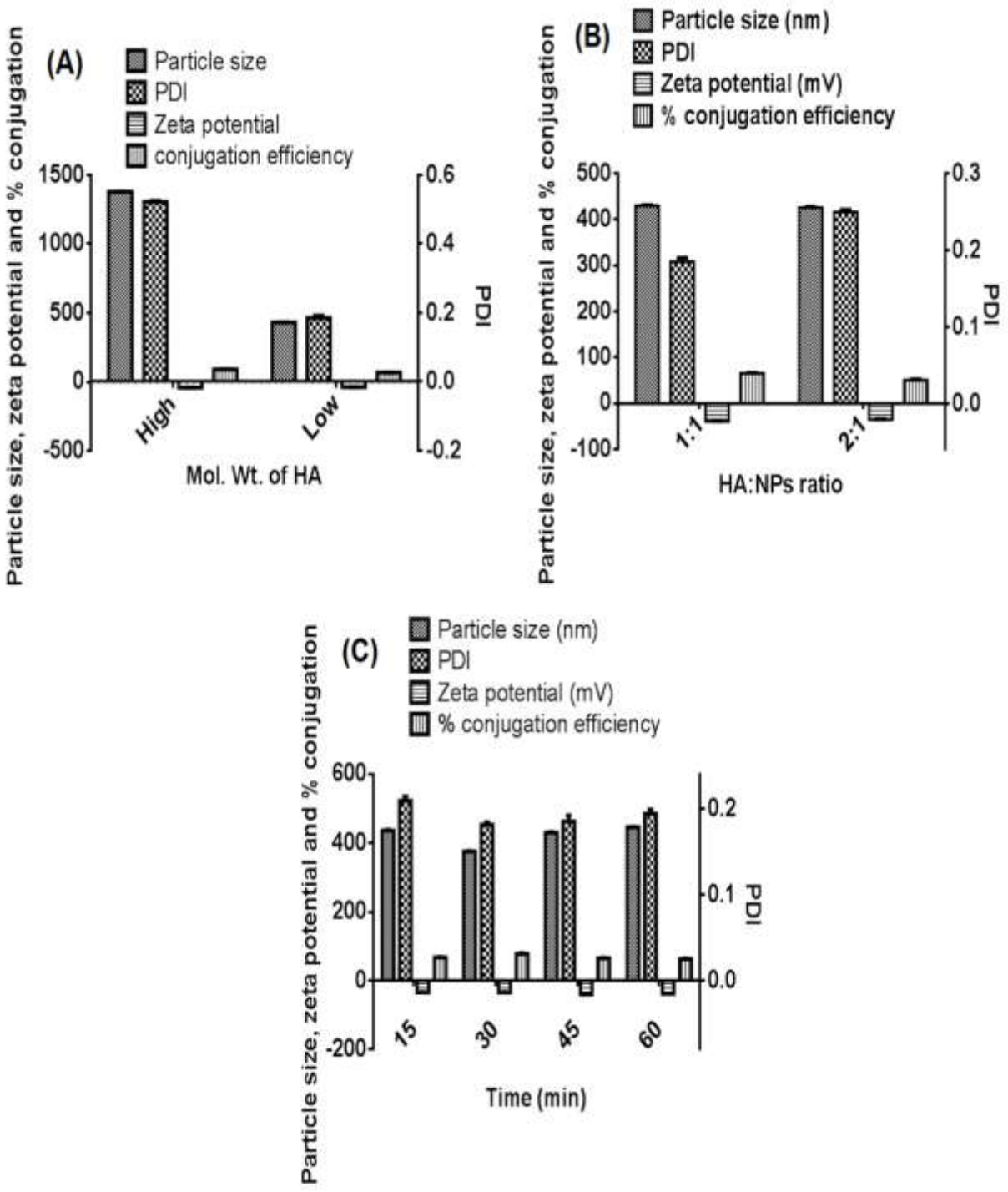

Figure 6.2: Optimization of HA-TNPs: (A) effect of molecular weight of HA on conjugation, (B) effect of HA : NPs ratio on conjugation and (C) effect of stirring time on conjugation. Data is represented as mean ± SD (n = 3).

6.4.2 Conjugation of CS with TNPs (CS-TNPs)

CS was also used to achieve CD44 mediated targeting of brain tumor and conjugated with TNPs by carbodiimide chemistry (figure 6.3). CS-TNPs optimization was done by varying single factor at a time and observed its effect on particle size, PDI, zeta potential and % conjugation efficiency of CS with the TNPs.

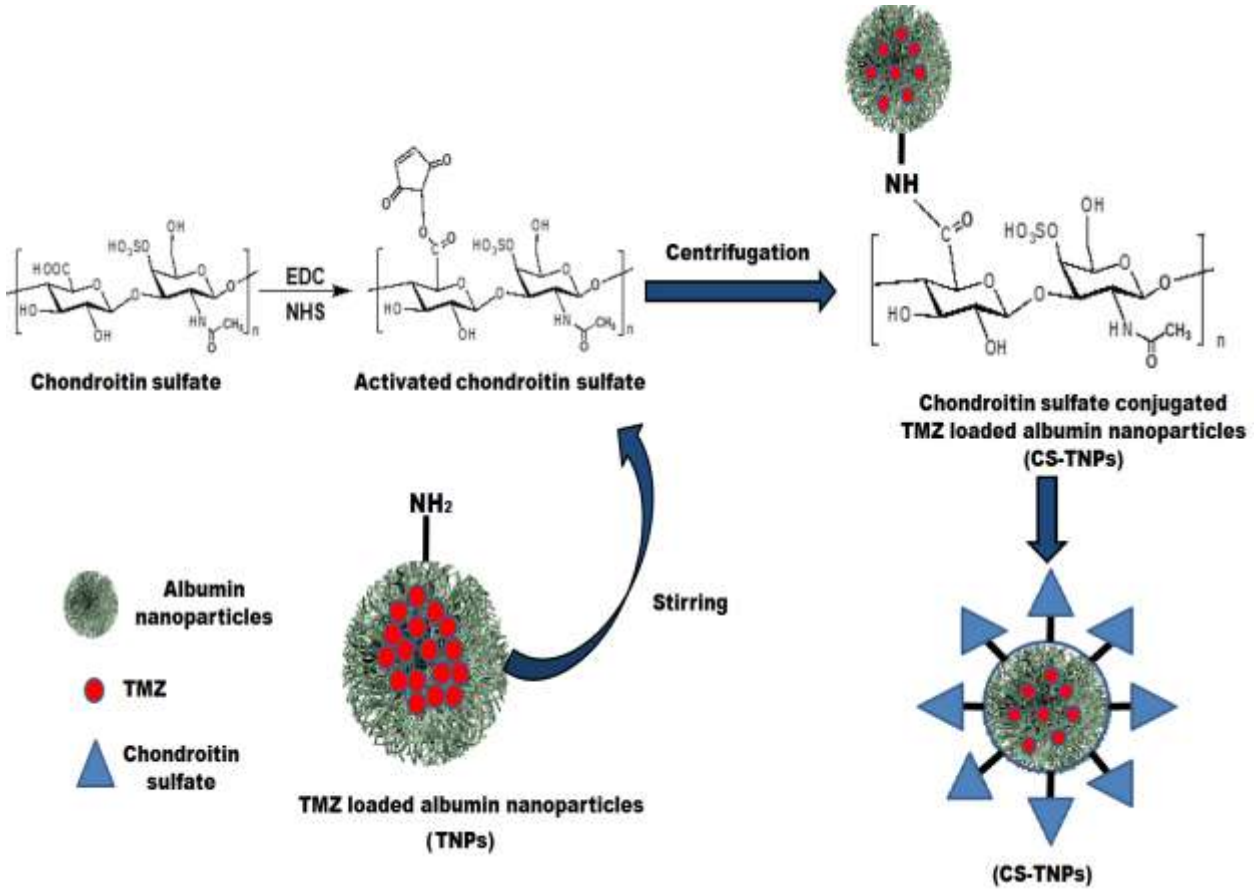

Figure 6.3 Schematic representation of fabrication of CS-TNPs

6.4.2.1 Effect of CS: NPs ratio on conjugation conjugation

Three different CS: NPs ratios were selected to optimize CS-TNPs viz. 1:1, 2:1 and 3:1. Obtained results are shown in table 6.4 and figure 6.4A. The results indicated that CS: NPs ratio does not have significant effect on particle size, PDI and zeta potential but has significant effect on conjugation efficiency. The insignificant effect of CS: NPs ratio on size, PDI and zeta potential may be correlated with the fact that after increasing the ratio, the surface area of

nanoparticles and the number of amine groups present on NPs (to bind with carboxylic groups of CS) remain constant. So, the size, PDI and zeta potential will not be affected to any large extent after increasing number of CS molecules but may affect conjugation efficiency. This may be attributed to the fact that with more the number of CS molecules more will be the chances of its conjugation on NPs and vice versa. So on the basis of higher conjugation efficiency, 1:1 was selected as CS: NPs ratio and used for further optimization.

Table 6.4: Effect of CS: NPs ratio on conjugation

CS: NPs ratio	Particle size (nm)	PDI	Zeta potential (mV)	% conjugation efficiency
1:1	190.9 ± 1.5	0.120 ± 0.005	-33.8 ± 0.5	71.6 ± 1.2
2:1	187.7 ± 1.75	0.143 ± 0.003	-34.5 ± 1.2	67.1 ± 1.9
3:1	205.6 ± 1.35	0.112 ± 0.007	-37.0 ± 0.6	62.2 ± 1.6

6.4.2.2 Effect of stirring time on conjugation

Effect of stirring time on the conjugation of CS was optimized on the basis of different stirring time (1 h, 2 h, 4 h and 12 h). Results indicated no significant effect of stirring time on particle size, PDI and zeta potential but had significant effect on % conjugation efficiency as shown in table 6.5 and figure 6.4B. As stirring time increased, % conjugation efficiency of CS with nanoparticles also increased. This may be correlated with the fact that as time passed, more interaction between carboxylic groups of activated CS and amine groups of albumin took place that led to enhancement of conjugation efficiency of CS with nanoparticles. So based upon these results, 12 h was selected as stirring time for conjugation.

Table 6.5: Effect of stirring time on conjugation

Time (h)	Particle size (nm)	PDI	Zeta potential (mV)	% conjugation efficiency
1	195.4 ± 1.5	0.214 ± 0.005	-40.0 ± 1.5	55.1 ± 1.6
2	197.1 ± 1.75	0.178 ± 0.003	-39.7 ± 1.2	63.3 ± 1.9
4	189.7 ± 1.35	0.181 ± 0.007	-39.2 ± 1.6	61.7 ± 1.5
12	190.9 ± 1.25	0.120 ±0.0048	-33.8 ± 1.1	71.6 ± 1.8

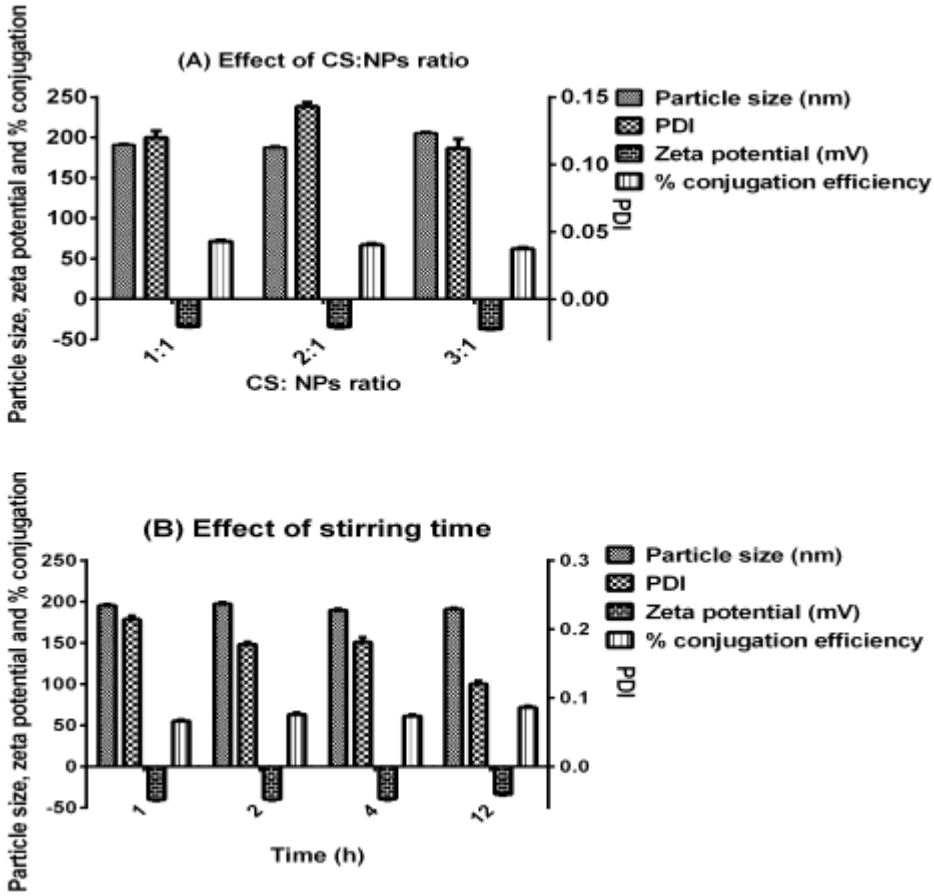

Figure 6.4: Optimization of CS-TNPs: (A) effect of CS: NPs ratio on conjugation and (B) effect of stirring time on conjugation. Data is represented as mean ± SD (n = 3)

Finally, it can be concluded that, for the conjugation of CS with TNPs, CS: NPs ratio 1 : 1 and 12 h stirring time were optimum and selected as optimized parameters for preparing final optimized CS-TNPs.

6.4.3 Characterization of surface modified TNPs (HA-TNPs and CS-TNPs)

6.4.3.1 Particle size and PDI determination

Particle size and PDI of HA-TNPs were found to be 375.1 ± 1.57 nm 0.181 ± 0.013 respectively (figure 6.5). In case of CS-TNPs, particles size and PDI was found to be 222.3 ± 1.57 nm and 0.217 ± 0.05 respectively (figure 6.6). In both HA-TNPs and CS-TNPs as compared to TNPs, increase in the particle size and PDI was observed which indicated conjugation of HA and CS with TNPs respectively (8,19).

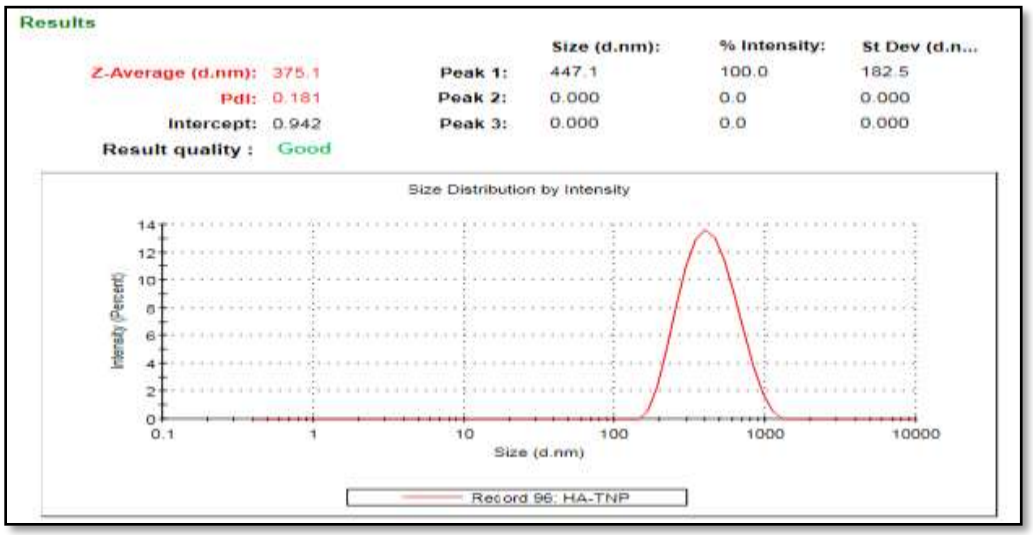

Figure 6.5 Particle size and PDI of HA-TNPs

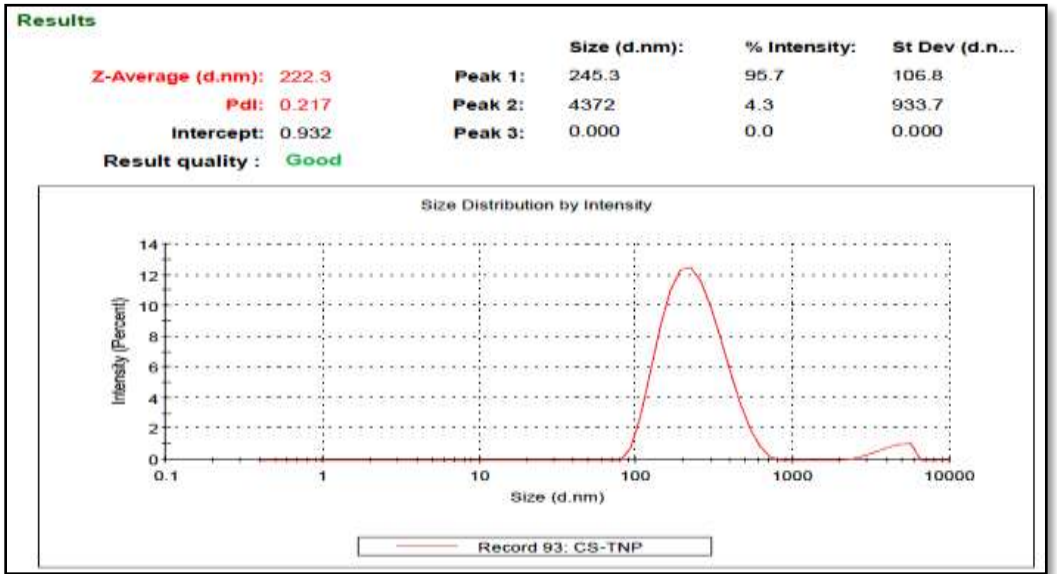

Figure 6.6 Particle size and PDI of CS-TNPs

6.4.3.2 Zeta potential determination

Zeta potential of HA-TNPs was observed as -33.6 ± 2.3 mV (figure 6.7). As discussed earlier, above pH 4.3, BSA showed negative zeta potential thus TNPs also showed negative zeta potential. In case of HA-TNPs, due to presence of HA (an anionic polymer containing carboxylic group), zeta potential was shifted towards more negative side. At pH 5.5, HA shows zeta potential value close to -30 mV and due to presence of HA, zeta potential of HA-TNPs also shifted towards -30 mV. The obtained results were also similar to previously reported literature (20). The value of zeta potential of TNPs and HA-TNPs indicated good colloidal stability.

In case of CS-TNPs, zeta potential was found to be -32.8 ± 1.87 mV (figure 6.8). As compared to TNPs, CS-TNPs showed higher negative zeta potential which was due to conjugation of CS with TNPs as CS contains various functional groups such as hydroxyl, carboxyl and sulphonic acid which impart negative charge on CS and due to this zeta potential of CS-TNPs shifted towards higher side. Zeta potential value of TNPs and CS-TNPs indicated stability of prepared nanoparticles as it may produce sufficient repulsion to overcome gravitational attraction between the nanoparticles and leads to better stability (19) .

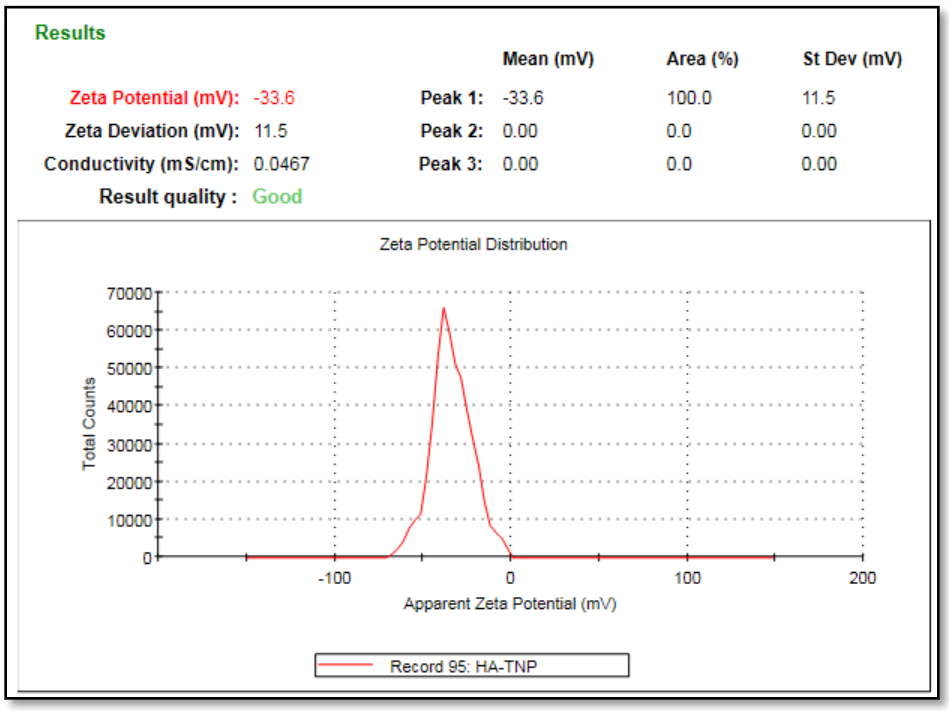

Figure 6.7 Zeta potential of HA-TNPs

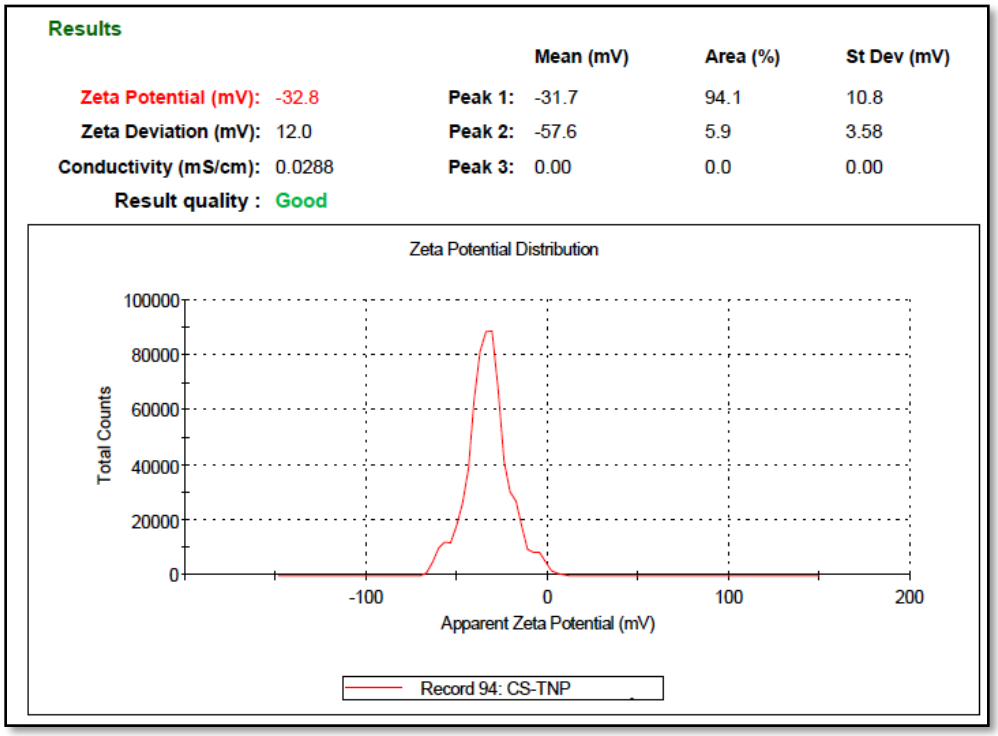

Figure 6.8: Zeta potential of CS-TNPs

6.4.3.3 DSC analysis

DSC thermograms of BSA, TMZ, PNPs, TNPs, HA-PNPs, HA-TNPs, CS-PNPs and CS-TNPs are shown in figure 6.9. As discussed earlier (section 5.4.4.3), the drug (TMZ) showed a sharp exothermic peak at 208.81^{o}C which indicates its crystalline nature of TMZ. Thermo gram of TNPs, HA-TNPs and CS-TNPs does not show any exothermic peak of TMZ which may be due to encapsulation of TMZ in the NPs in form of molecular dispersion (7).

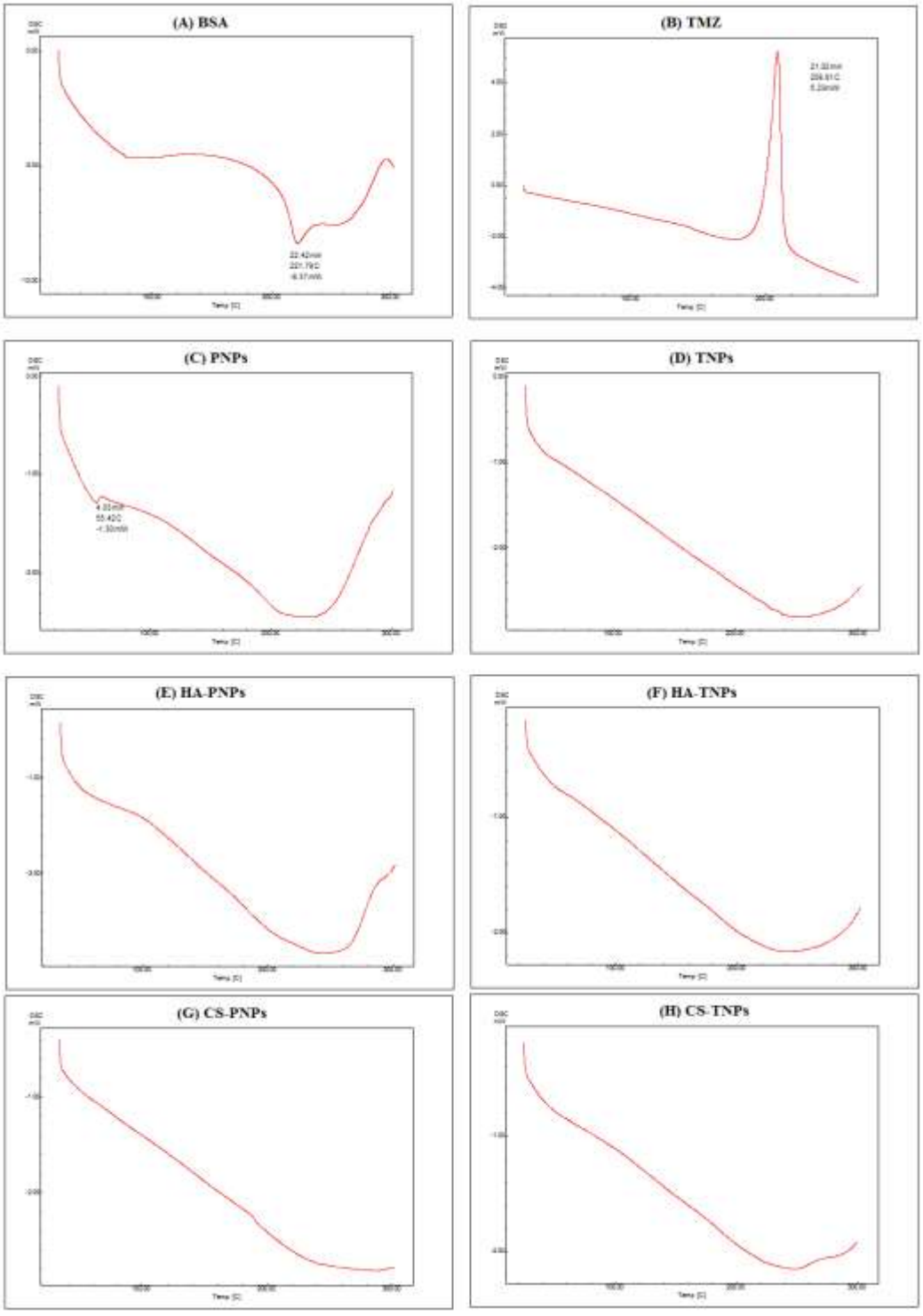

Figure 6.9: DSC thermograms of (A) BSA, (B) TMZ, (C) PNPs, (D) TNPs, (E) HA-PNPs, (F) HA-TNPs, (G) CS-PNPs and (H) CS-TNPs

6.4.3.4 FTIR analysis

FTIR spectrum of BSA, HA, CS, TMZ, PNPs, TNPs, HA-TNPs and CS-TNPs are shown in figure 6.10. Pure TMZ shows characteristic peaks at 3419.79 cm^{-1} and 3385.07 cm^{-1} [–N-H stretch for amines], 3113.11 cm^{-1}, 3184.48 cm^{-1} and 3284.77 cm^{-1} [the =C-H- (alkene) stretch], 1757.15 cm^{-1}, 1730.15 cm^{-1} and1674.21 cm^{-1} [–C=O stretch contributed by aldehydes, ketones or amide group], 1598.99 cm^{-1} and 1674.21 cm^{-1} [–C=C- (Alkene) stretch] and 1360 cm^{-1} to 1180 cm^{-1} can be attributed to -C-N stretch from amines. Spectrum of BSA showed characteristic peaks at 3277.06 cm^{-1}[–NH stretching vibration], 2873 -2950 cm^{-1} [-C-H and -C-H methoxy stretching vibration], 1641.42 cm^{-1}[-C=O stretching vibrations of amide] and 1535.34 cm^{-1}[-N–H bending -C–N stretching vibration of amide]. FTIR spectrum of HA showed characteristic peaks at 3374 cm^{-1} [-OH stretching], ~1550-1560 cm^{-1} [amide II -N-H band], 1604.77 cm^{-1} and ~1400 cm^{-1} [-C=O stretching vibration]. FTIR spectrum of CS showed characteristic peaks at 3340.71 cm^{-1} {-OH stretching}, ~1562.34 cm^{-1} {amide II -N-H band}, 1612.49 cm^{-1} and ~1408.04 cm^{-1} {-C=O stretching vibration}. In case of PNPs, all characteristic peaks of BSA were present with lesser intensity as compared to pure BSA. In case of TNPs and HA-TNPs, all characteristic peaks of BSA, HA and TMZ were present but the intensity of TMZ characteristic peaks were decreased which indicates that TMZ was present as amorphous form in TNPs and HA-TNPs (7,8). In case of CS-TNPs, new peaks at 1527.62 cm-1 {attributed to amide bond}, 3307.92 cm-1 and 1450.47 cm-1{for–NH and CN group} were observed which confirmed the conjugation of CS with TNPs (7,19).

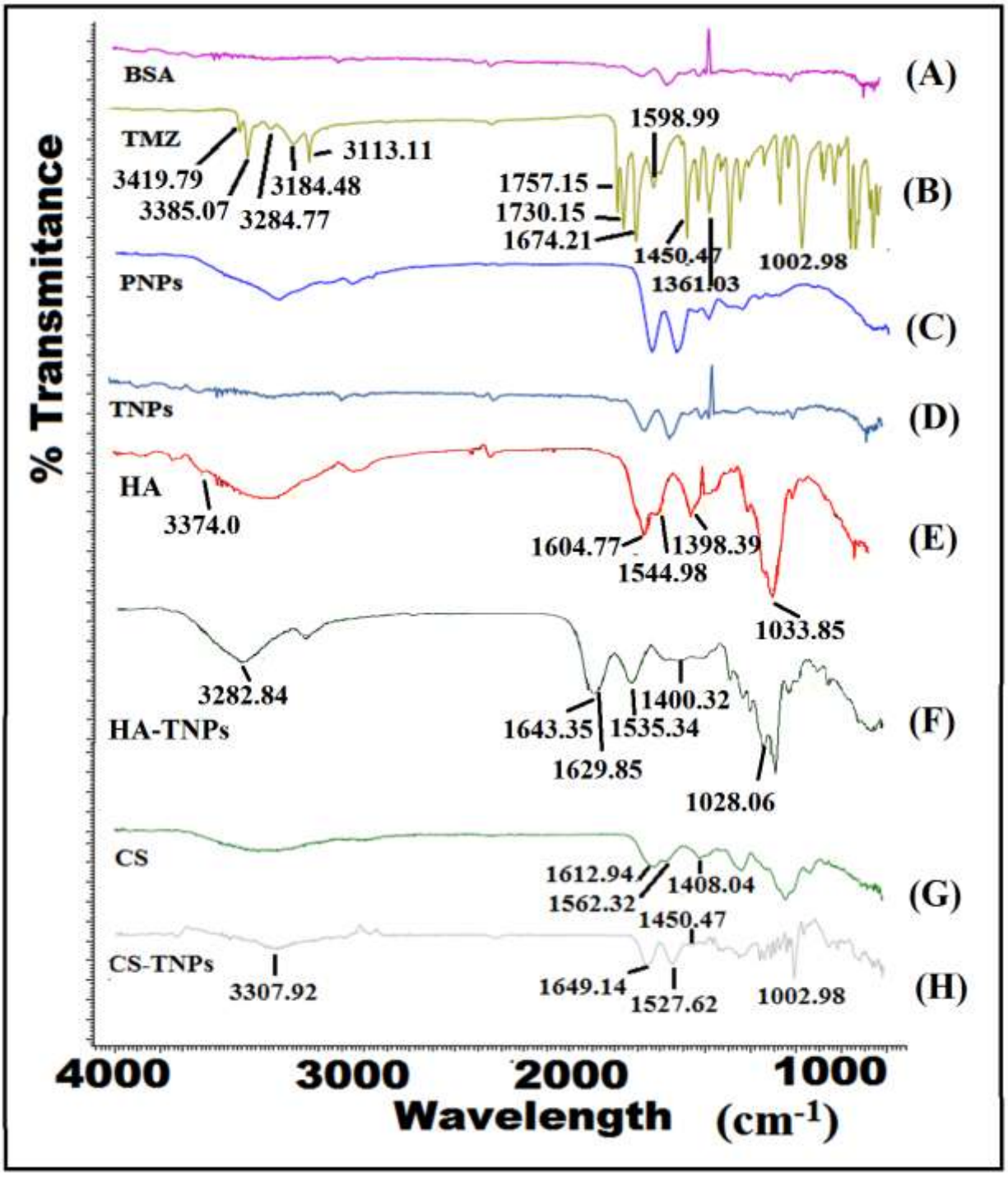

Figure 6.10: FTIR spectrums of (A) BSA, (B) TMZ, (C) PNPs, (D) TNPs, (E) HA, (F) HA-TNPs, (G) CS and (CS-TNPs)

6.4.3.5 XRD analysis

X-ray diffractograms (XRD) of pure TMZ, BSA, PNPs, TNPs, HA-PNPs, HA-TNPs, CS-PNPs and CS-TNPs are shown in figure 6.11. TMZ showed characteristic sharp and intense peaks at 2θ values of 10.7°, 14.64°, 26.4° and 28.2° indicative of highly crystalline nature of drug. XRD pattern of BSA did not show any sharp peaks representing its amorphous nature. The hollow pattern of PNPs, HA-PNPs and CS-PNPs indicated that the formed nanoparticles were amorphous. XRD pattern of TNPs and HA-TNPs were also similar to blank nanoparticles (PNPs and HA-PNPs) indicating the probability of most of the drug getting entrapped in the polymeric matrix of the nanoparticles as sharp peaks of TMZ were not seen in drug loaded nanoparticles In diffractogram of CS-TNPs, characteristic peaks of TMZ were present but their intensity was decreased. This may be due to conversion of crystalline TMZ into amorphous form after encapsulating in the nanoparticles (7). Apart from this, some additional peaks were also present which may be due to trehalose. The conversion of crystalline TMZ into amorphous TMZ after encapsulating in nanoparticles may also beneficial in terms of solubility and bioavailability as amorphous form is more soluble as compare to crystalline.

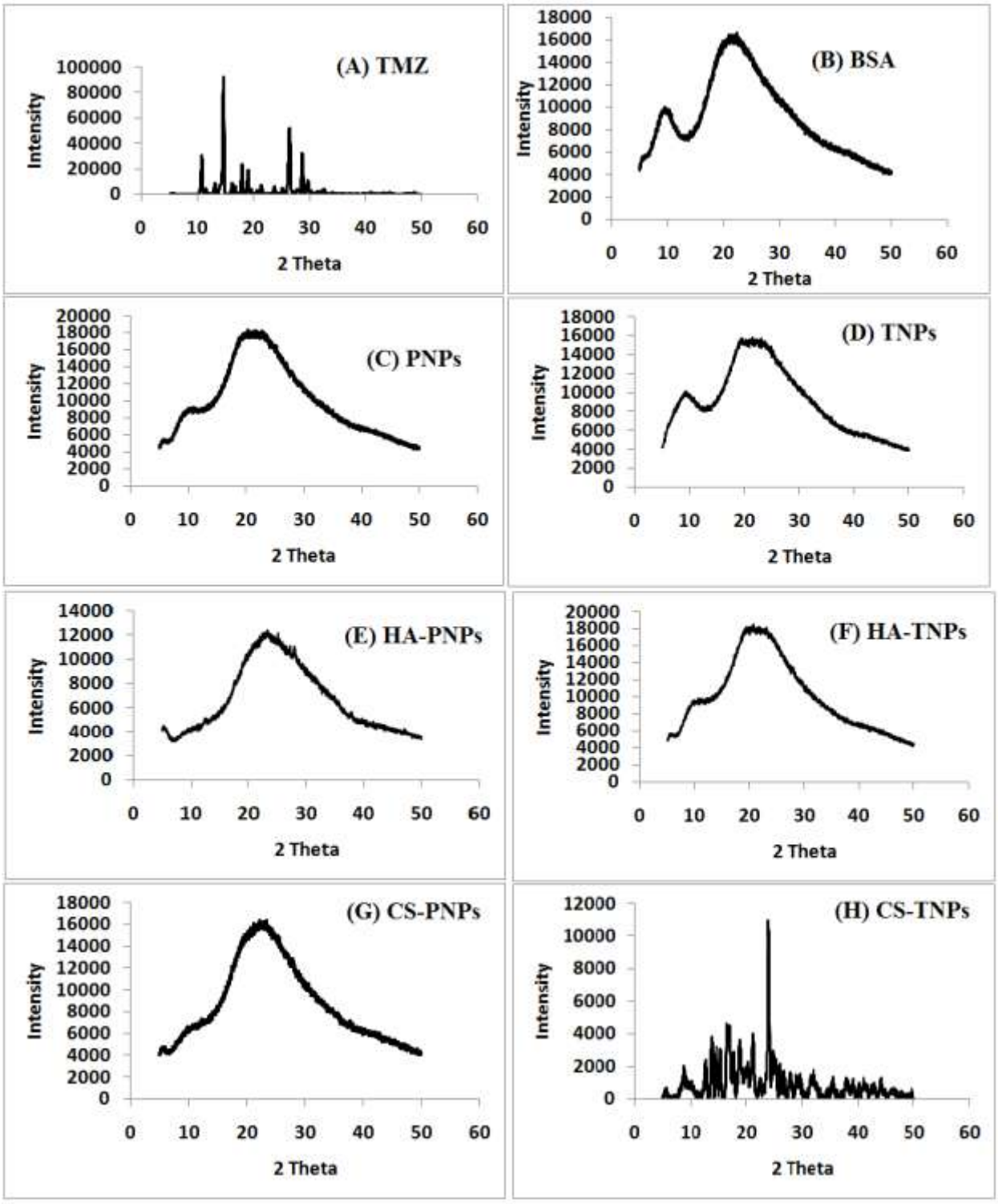

Figure 6.11: XRD diffractograms of (A) BSA, (B) TMZ, (C) PNPs, (D) TNPs, (E) HA-PNPs (F) HA-TNPs, (G) CS-PNPs and (H) CS-TNPs

6.4.3.6 Morphology

Morphology of TNPs, HA-TNPs and CS-TNPs were determined by TEM analysis. TEM image of TNPs and HA-TNPs showed roughly spherical shape (figure 6.12 A and B respectively) while CS-TNPs showed spherical shape (figure 6.12 C). TEM image of HA-TNPs and CS-TNPs exhibited a dark core surrounded by a lighter gray rim likely corresponding to the HA and CS conjugation. Size of TNPs, HA-TNPs and CS-TNPs obtained by TEM was lower than that obtained by zetasizer (DLS measurement). Higher particle size in case of DLS may be due to the presence of hydration layer while in case of TEM, size was measured in dried state [14].

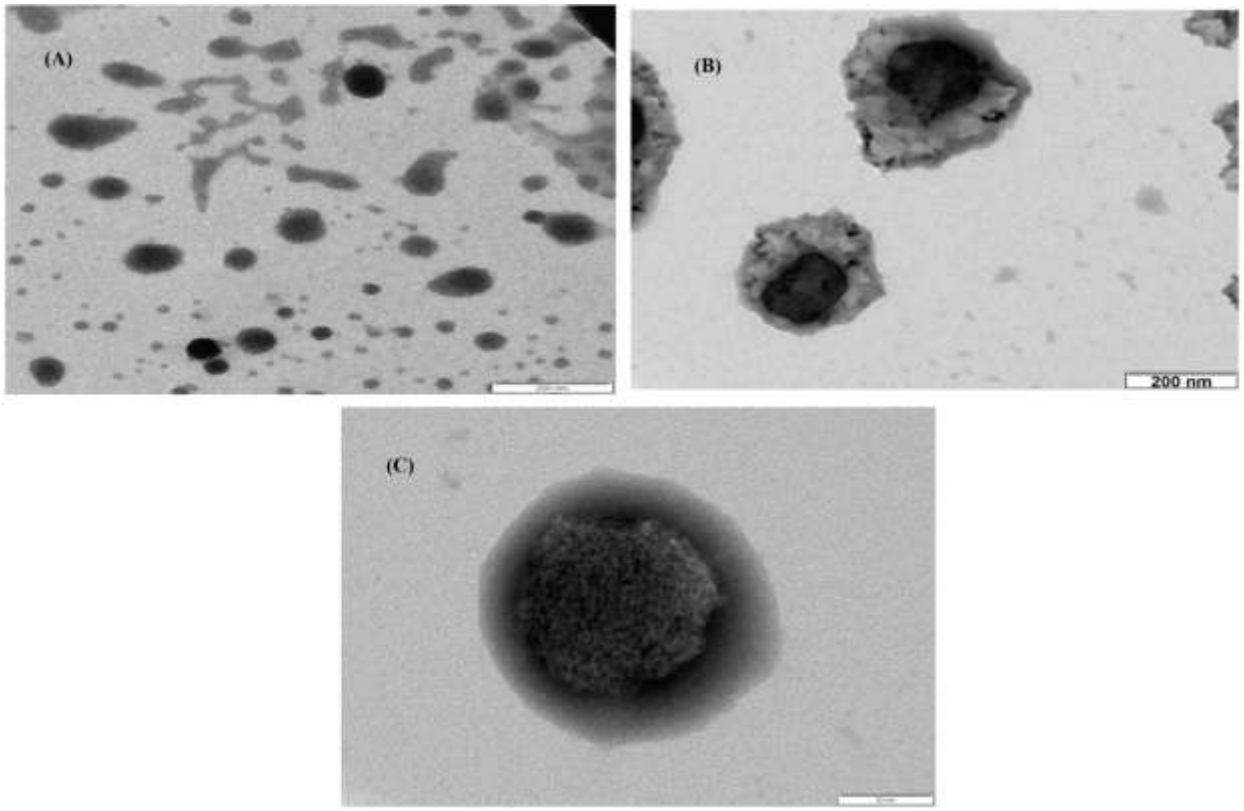

Figure 6.12: TEM image of (A) TNPs, (B) HA-TNPs and (C) CS-TNPs

6.4.3 Evaluation of HA-TNPs

6.4.3.1 Estimation of entrapment efficiency and drug loading

Percent entrapment efficiency of final optimized HA-TNPs was found to be 64.29 % ± 3.51 % while percent drug loading was found to be 4.51 % ± 1.57 %. In case of CS-TNPs, the percent entrapment efficiency was found to be 61.68 % ± 3.5 % while percent drug loading was found to

be 4.32 % ± 0.9 %. As compared to TNPs, the decrease in the % EE of HA-TNPs and CS-TNPs may be correlated with the fact that some amount of entrapped TMZ in TNPs may get released during conjugation of HA/CS with TNPs as the conjugation reaction took place in the aqueous condition for 30 min (HA-TNPs) and 12 h (CS-TNPs) respectively. The decrease in the % DL can be correlated with the fact that in case of HA-TNPs and CS-TNPs, total weight of the nanoparticles increased as compared to TNPs which led to reduction in the % DL because total weight of nanoparticles is inversely proportional to % DL.

6.4.3.2 *In-vitro* drug release

The cumulative *in-vitro* drug release (% CDR) from TMZ, TNPs, HA-TNPs and CS-TNPs was demonstrated at pH 5.5 ± 0.2 to mimic tumor environment. The results of in-vitro drug release from TMZ, TNPs, HA-TNPs and CS-TNPs (figure 6.13) indicated almost 100% drug release of pure TMZ within 1.5 h while only 43.81% ± 1.30%, 32.03% ± 1.50% and 26.63 % ± 1.50 % drug was released after 2 h from TNPs, HA-TNPs and CS-TNPs respectively. From TNPs 56.68% ± 1.48% and 61.12% ± 1.56% drug release was observed after 24 h and 48 h respectively while from HA-TNPs only 42.78% ± 1.56% and 46.10% ± 1.52% drug release was observed after 24 h and 48 h respectively. In case of CS-TNPs, only 32.53 % ± 1.51 % and 42.42 % ± 1.54 % drug release was observed after 24 h and 48 h respectively. Slower release from HA-TNPs and CS-TNPs may be due to conjugation of HA / CS over the surface of TNPs which may act as a barrier to release drug from nanoparticles. A biphasic release pattern of TMZ was observed from developed TNPs, HA-TNPs and CS-TNPs characterized by an initial rapid release within half an hour, followed by slower and sustained release. The slower and sustained release behavior of drug may be due to slow diffusion of drug from entrapped BSA and HA/CS conjugated BSA (21).

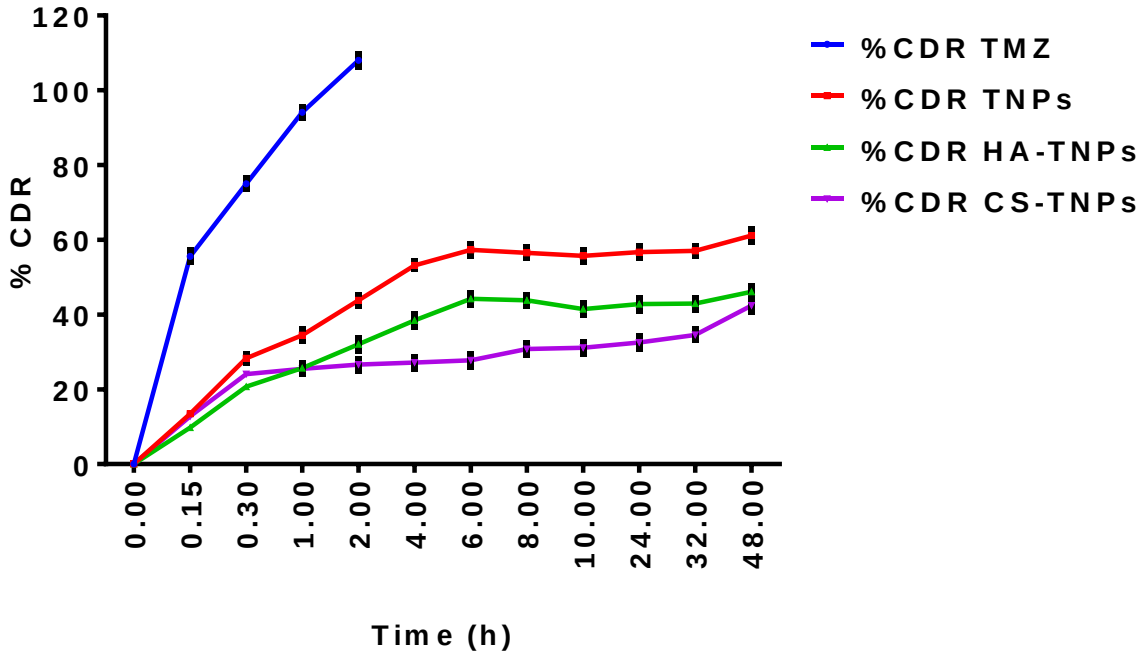

Figure 6.13: In vitro drug release study of TMZ, TNPs, HA-TNPs and CS-TNPs in sodium acetate buffer pH 5.5

6.4.7 Bio-interaction studies

The interaction of HA-TNPs and CS-TNPs with plasma protein, cell culture media, serum proteins and RBCs were performed to evaluate the change in surface conditions of HA-TNPs and CS-TNPs in existence of mentioned biological factors.

6.4.7.1 Interaction with plasma proteins

The interaction of HA-TNPs and CS-TNPs with plasma protein was performed and results indicated no significant interaction between plasma proteins as no significant change in zeta potential and particle size was observed. Initial particle size and zeta potential of HA-TNPs were 375.7 ± 5.3 nm and -33.6 ± 1.7 mV respectively while after interaction with plasma proteins the obtained particle size and zeta potential were 371.5 ± 1.7 nm and -32.9 ± 2.9 mV respectively. In case of CS-TNPs, initial particle size and zeta potential was 222.3 ± 1.6 nm and -32.8± 1.9

respectively while after interaction with plasma proteins the obtained particle size and zeta potential were 225.5 ± 1.3 nm and -31.9 ± 2.1 mV respectively. Hence it may conclude that the developed HA-TNPs and CS-TNPs can act as an efficient platform for targeting tumor without trailing its surface functionality.

6.4.7.2 Interaction with cell culture medium

The interaction of HA-TNPs and CS-TNPs with cell culture media (DMEM) was performed and results indicated no significant interaction between DMEM as no significant change in particle size and zeta potential was observed. Initial particle size and zeta potential of HA-TNPs were 375.7 ± 5.3 nm and -33.6 ± 1.7 mV respectively while after interaction with DMEM media obtained particle size and zeta potential were 371.5 ± 2.8 nm and -33.4 ± 1.3 mV respectively. In case of CS-TNPs, initial particle size and zeta potential was 222.3 ± 1.6 nm and -32.8± 1.9 respectively while after interaction with DMEM media, the obtained particle size and zeta potential were 227.5 ± 2.3 nm and -32.5 ± 1.3 mV respectively. Hence it may be concluded that the developed HA-TNPs and CS-TNPs were stable in cell culture media (DMEM).

6.4.7.3 Interaction with serum

The interaction of HA-TNPs and CS-TNPs with serum was performed and results demonstrated no significant interaction between serum proteins as no significant change in particle size and zeta potential was observed. Initial particle size and zeta potential of HA-TNPs were 375.7 ± 5.3 nm and -33.6 ± 1.7 mV respectively while after interaction with DMEM media obtained particle size and zeta potential were 377.5 ± 3.1 nm and -32.9 ± 2.3 mV respectively. In case of CS-TNPs, initial particle size and zeta potential was 222.3 ± 1.6 nm and -32.8± 1.9 respectively while after interaction with the serum obtained particle size and zeta potential were 224.5 ± 2.7 nm and -31.5 ± 2.1 mV respectively. Hence it may be concluded that the developed HA-TNPs and CS-TNPs were stable in serum.

6.4.7.4 Haemolysis studies

Haemolysis study was performed for developed HA-TNPs and CS-TNPs. The absorbance values were obtained by scanning the samples by UV-Visible spectrophotometer and the percent

haemolysis was calculated on the basis of equation 6.3. The absorbance for positive control (Triton X- 100) and negative control (DMSO) was found to be 0.669 and 0.152 respectively. The % haemolysis for both HA-TNPs and CS-TNPs were found to be 1.35 % ± 0.01 % and 1.16 % ± 0.03 % respectively corresponding to absorbance values 0.159 and 0.158 respectively. The results demonstrated no significant haemolysis potential of developed HA-TNPs and CS-TNPs as the % haemolysis for both HA-TNPs and CS-TNPs were found to be less than 2 (13) .

6.4.8 Stability studies

The results of stability studies (Table 6.6 and 6.7) indicated that prepared HA-TNPs and CS-TNPs were stable at both refrigerated condition and room temperature (25°C) for three months as no significant change in particle size, assay and zeta potential was observed.

Table 6.6: Stability studies of lyophilized HA-TNPs. Data is represented as mean ± SD (n=3)

Time (month)	Particle size (nm)	Zeta potential (mV)	% EE	% Assay
	HA-TNPs	HA-TNPs	HA-TNPs	HA-TNPs
At refrigerated condition (4 °C)				
0	375.1± 1.57	-33.6± 2.3	64.29% ± 3.51%	100 % ± 1.3 %
1	375.5 ± 3.81	-32.6± 1.5	64.67% ± 2.53%	99.4 % ± 4.3 %
2	374.8 ± 4.91	-32.3 ± 1.2	63.71% ± 2.91%	98.5 % ± 3.3 %
3	377.5 ± 5.65	-31.9 ± 0.9	63.23% ± 3.13%	97.7 % ± 4.5 %
At room temperature (25°C ±2°C and 65% ± 5% relative humidity)				
0	375.1± 1.57	-33.6± 2.3	64.29% ± 3.51%	100.0 % ± 1.9 %
1	375.6 ± 7.67	-32.4 ± 1.5	64.88% ± 3.23%	99.1 % ± 4.9 %
2	376.1 ± 9.35	-31.6± 1.3	63.54% ± 2.97%	97.0 % ± 3.7 %
3	377.5 ± 10.87	-30.8 ± 1.1	63.05% ± 3.19%	96.2 % ± 4.9 %

Table 6.7: Stability studies of lyophilized CS-TNPs. Data is represented as mean ± SD (n=3)

Time (month)	Particle size (nm)	Zeta potential (mV)	% Assay
	CS-TNPs	**CS-TNPs**	**CS-TNPs**
At refrigerated condition (4 °C)			
0	222.3 ± 1.57	-32.8 ± 1.87	100.0 ± 1.50
1	225.5 ± 3.81	-31.6 ± 1.31	99.22 ± 2.93
2	228.8 ± 5.87	-31.3 ± 1.05	98.43 ± 2.99
3	230.5 ± 7.53	-30.5 ± 1.49	97.49 ± 3.81
At room temperature (25°C ±2°C and 65% ± 5% relative humidity)			
0	222.3 ± 1.57	-32.8 ±1.87	100.0 ± 1.50
1	227.6 ± 4.67	-31.4 ± 1.51	98.70 ± 3.47
2	232.1 ± 7.35	-30.6 ± 1.35	98.15 ± 3.83
3	238.5 ± 9.93	-30.1 ± 1.50	97.37 ± 4.79

References

1. Oueslati N, Leblanc P, Harscoat-Schiavo C, Rondags E, Meunier S, Kapel R, et al. CTAB turbidimetric method for assaying hyaluronic acid in complex environments and under cross-linked form. Carbohydr Polym. 2014 Nov 4;112:102–8.

2. Qhattal HSS, Liu X. Characterization of CD44-mediated cancer cell uptake and intracellular distribution of hyaluronan-grafted liposomes. Mol Pharm. 2011 Aug 1;8(4):1233–46.

3. Bishnoi M, Jain A, Hurkat P, Jain SK. Aceclofenac-loaded chondroitin sulfate conjugated SLNs for effective management of osteoarthritis. J Drug Target. 2014 Nov;22(9):805–12.

4. Anhorn MG, Mahler H-C, Langer K. Freeze drying of human serum albumin (HSA) nanoparticles with different excipients. Int J Pharm. 2008 Nov;363(1–2):162–9.

5. Kamali M, Dinarvand R, Maleki H, Arzani H, Mahdaviani P, Nekounam H, et al. Preparation of imatinib base loaded human serum albumin for application in the treatment of glioblastoma. RSC Adv. 2015 Jul 16;5(76):62214–9.

6. Lo Y-L, Chou H-L, Liao Z-X, Huang S-J, Ke J-H, Liu Y-S, et al. Chondroitin sulfate-polyethylenimine copolymer-coated superparamagnetic iron oxide nanoparticles as an efficient magneto-gene carrier for microRNA-encoding plasmid DNA delivery. Nanoscale. 2015 May 14;7(18):8554–65.

7. Jain D, Bajaj A, Athawale R, Shrikhande S, Goel PN, Nikam Y, et al. Surface-coated PLA nanoparticles loaded with temozolomide for improved brain deposition and potential treatment of gliomas: development, characterization and in vivo studies. Drug Deliv. 2016;23(3):999–1016.

8. Huang D, Chen Y-S, Rupenthal ID. Hyaluronic Acid Coated Albumin Nanoparticles for Targeted Peptide Delivery to the Retina. Mol Pharm. 2017 06;14(2):533–45.

9. Fang C, Wang K, Stephen ZR, Mu Q, Kievit FM, Chiu DT, et al. Temozolomide nanoparticles for targeted glioblastoma therapy. ACS Appl Mater Interfaces. 2015 Apr 1;7(12):6674–82.

10. Song Z, Lu Y, Zhang X, Wang H, Han J, Dong C. Novel curcumin-loaded human serum albumin nanoparticles surface functionalized with folate: characterization and in vitro/vivo evaluation. Drug Des Devel Ther. 2016;10:2643–9.

11. Katas H, Hussain Z, Awang SA. Bovine Serum Albumin-Loaded Chitosan/Dextran Nanoparticles: Preparation and Evaluation of Ex Vivo Colloidal Stability in Serum [Internet]. Vol. 2013, Journal of Nanomaterials. Hindawi; 2013 [cited 2020 Oct 6]. p. e536291. Available from: https://www.hindawi.com/journals/jnm/2013/536291/

12. Pandey A, Singh K, Patel S, Singh R, Patel K, Sawant K. Hyaluronic acid tethered pH-responsive alloy-drug nanoconjugates for multimodal therapy of glioblastoma: An intranasal route approach. Mater Sci Eng C Mater Biol Appl. 2019 May;98:419–36.

13. Zhang G-S, Hu P-Y, Li D-X, He M-Z, Rao X-Y, Luo X-J, et al. Formulations, Hemolytic and Pharmacokinetic Studies on Saikosaponin a and Saikosaponin d Compound Liposomes. Molecules. 2015 Apr;20(4):5889–907.

14. Yadav AK, Agarwal A, Rai G, Mishra P, Jain S, Mishra AK, et al. Development and characterization of hyaluronic acid decorated PLGA nanoparticles for delivery of 5-fluorouracil. Drug Deliv. 2010 Nov;17(8):561–72.

15. Bharti N, Harikumar SL, Buddiraja A. Development and characterization of albumin nanoparticles for pulmonary drug delivery. :7.

16. Chitkara D, Kumar N. BSA-PLGA-based core-shell nanoparticles as carrier system for water-soluble drugs. Pharm Res. 2013 Sep;30(9):2396–409.

17. Abraham J. International Conference On Harmonisation Of Technical Requirements For Registration Of Pharmaceuticals For Human Use. In: Tietje C, Brouder A, editors. Handbook of Transnational Economic Governance Regimes [Internet]. Brill | Nijhoff; 2010 [cited 2020 Sep 5]. p. 1041–53. Available from: https://brill.com/view/book/edcoll/9789004181564/Bej.9789004163300.i-1081_085.xml

18. He M, Zhao Z, Yin L, Tang C, Yin C. Hyaluronic acid coated poly(butyl cyanoacrylate) nanoparticles as anticancer drug carriers. Int J Pharm. 2009 May 21;373(1–2):165–73.

19. Liu P, Chen N, Yan L, Gao F, Ji D, Zhang S, et al. Preparation, characterisation and in vitro and in vivo evaluation of CD44-targeted chondroitin sulphate-conjugated doxorubicin PLGA nanoparticles. Carbohydr Polym. 2019 Jun 1;213:17–26.

20. Edelman R, Assaraf YG, Levitzky I, Shahar T, Livney YD. Hyaluronic acid-serum albumin conjugate-based nanoparticles for targeted cancer therapy. Oncotarget. 2017 Apr 11;8(15):24337–53.

21. Bagari R, Bansal D, Gulbake A, Jain A, Soni V, Jain SK. Chondroitin sulfate functionalized liposomes for solid tumor targeting. J Drug Target. 2011 May 1;19(4):251–7.